
When Are Experts Misrouted? Counterfactual Routing Analysis in Mixture-of-Experts Language Models

Youngsik Yoon¹ Siwei Wang³ Wei Chen³ Jungseul Ok^{1,2*}

¹Department of Computer Science and Engineering, POSTECH, South Korea

²Graduate School of Artificial Intelligence, POSTECH, South Korea

³Microsoft Research Asia, Beijing, China

{ysyoon97, jungseul.ok}@postech.ac.kr, {siweiwang, weic}@microsoft.com

Abstract

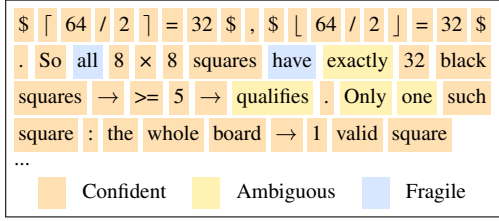
Mixture-of-Experts (MoE) language models route each token to a small subset of experts, but whether the routes selected by a trained top- k router are good ones is rarely evaluated directly. Holding the model fixed, we compare each standard route against sampled equal-compute alternatives for the same token and score each by the next-token probability it assigns to the realized token in a verified reasoning trajectory. The result is sharply token-conditional: the standard router is well-aligned with route utility on confident tokens but uninformative on the fragile tokens that drive hard reasoning, where lower-loss equal-compute routes consistently exist inside the frozen model but are not selected. The same pattern holds across Qwen3-30B-A3B, GPT-OSS-20B, DeepSeek-V2-Lite, and OLMoE-1B-7B, and follows structurally from how standard top- k training evaluates routing decisions: the language modeling loss scores only the executed route, and load balancing depends only on aggregate routing statistics. A minimal router-only update to the final-layer router, leaving every expert and every other router frozen, is sufficient to shift pass@K on AIME 2024+2025 and HMMT 2025 for both Qwen3-30B-A3B and GPT-OSS-20B, suggesting that at least part of the failure reflects router-reachable misallocation rather than expert capacity alone.

1 Introduction

Mixture-of-Experts (MoE) language models provide an efficient way to scale model capacity by activating only a small subset of parameters for each token. By routing each token to a few experts rather than executing the full model, sparse MoE models can scale total parameters while keeping per-token compute roughly fixed (Shazeer et al., 2017; Lepikhin et al., 2020; Fedus et al., 2022; Du et al., 2022). This design has become a common choice in recent frontier and open-weight language models, including Mixtral (Jiang et al., 2024), DeepSeek-V3/R1 (Liu et al., 2024b; Guo et al., 2025), Qwen3 (Yang et al., 2025), and GPT-OSS (Agarwal et al., 2025).

The component that decides which experts process each token is the router, typically a single learned linear projection followed by top- k selection over experts. Compared with the attention and expert components, the router has received relatively little attention: standard MoE pretraining treats routing as a balanced-allocation problem solved by load-balancing (Shazeer et al., 2017; Fedus et al., 2022) and stability regularizers (Zoph et al., 2022), with downstream performance taken as sufficient evidence of good routing. Analyses of trained routers report that routing stabilizes early and exhibits structured specialization (Dai et al., 2022; Xue et al., 2024), properties read as the router doing its job, and the apparent adequacy of these routers is rarely questioned in subsequent analysis.

*Corresponding author.



(a) Confidence along a reasoning trace.

Confidence	Confident	Ambiguous	Fragile
	$\bar{p} > 0.9$	$0.9 \geq \bar{p} > 0.5$	$0.5 \geq \bar{p}$
Tokens (%)	78.7	14.3	6.9
Top-1 (%)	51.9	1.5	0.8
p_{std} (%)	99.6	77.9	40.2
p_{best} (%)	99.8	88.9	60.6
Gap (pp)	0.2	11.0	20.4

(b) Routing gaps by confidence bin.

Figure 1: **Counterfactual routing statistics by confidence bin.** Tokens are grouped by \bar{p} , the mean realized-token probability over sampled equal-compute alternative routes: Confident ($\bar{p} > 0.9$), Ambiguous ($0.5 < \bar{p} \leq 0.9$), and Fragile ($\bar{p} \leq 0.5$). Top-1 reports how often the standard top- k route is best among evaluated routes. p_{std} and p_{best} denote realized-token probabilities under the standard and best evaluated routes, and Gap is their difference. Results are for Qwen3-30B-A3B at the final MoE layer on verified MATH Level-5 trajectories.

We ask whether, in MoE language models, the routing decisions actually made by the standard top- k router are good ones. Holding the model fixed, we compare each standard top- k route against sampled equal-compute alternatives of the same size and score each route by the next-token probability it assigns to the realized token in a verified reasoning trajectory. This question is especially important at low-confidence reasoning tokens. Prior work shows that reasoning success can depend disproportionately on a small subset of pivotal, critical, or high-entropy tokens (Abdin et al., 2024; Lin et al., 2024; Wang et al., 2025). We therefore group tokens by counterfactual confidence: the average probability assigned to the realized next token by sampled alternative routes.

Figure 1 shows the core pattern. On Confident tokens, the standard route is often the best evaluated route and closely matches the best sampled route in next-token probability. On Fragile tokens, this alignment collapses: the standard route is best on only 0.8% of tokens, while the best sampled equal-compute route improves next-token probability by 20.4 percentage points. Thus the failure is not uniform routing noise; it concentrates on the low-confidence tokens where route choice is most consequential. The same pattern holds across layers, benchmarks, and MoE model families.

The misalignment we observe is consistent with a structural property of standard top- k MoE training: the language modeling loss only evaluates the route that was executed, while load balancing and other auxiliary losses depend only on aggregate router-side statistics, not on the loss that would have resulted from a different route on the same token.

We then test whether this routing failure is partially reachable inside the frozen trained model. Updating only the final-layer router with counterfactual route preferences, while freezing all experts and earlier-layer routers (less than 0.001% of model parameters), is sufficient to shift pass@K on AIME 2024+2025 and HMMT 2025 for both Qwen3-30B-A3B and GPT-OSS-20B. That such a small router-only update shifts downstream performance supports the reading that some high-loss predictions on hard tokens reflect a routing failure rather than a pure capacity limit.

In summary, this paper provides a counterfactual analysis of routing quality in trained MoE language models, showing that the standard router can be well-aligned on confident tokens but systematically misaligned on harder ones, and that this misalignment is partially reachable through a minimal router-only update. Our results suggest that routing quality should be considered as a first-class concern in MoE training, not just as an implementation detail of sparsity.

2 Preliminaries

A sparse MoE layer replaces a single dense feed-forward block with N parallel expert modules $\{E_i\}_{i=1}^N$, each $E_i : \mathbb{R}^d \rightarrow \mathbb{R}^d$, and routes each token to a small subset of them. Let $x_t \in \mathbb{R}^d$ denote the hidden representation of token position t entering the layer, where d is the model width.

The routing decision is made by a learned linear router with weights $W_r \in \mathbb{R}^{N \times d}$ and bias $b_r \in \mathbb{R}^N$, which produces a vector of expert scores $s_t = W_r x_t + b_r \in \mathbb{R}^N$, where s_{ti} is the score assigned to expert i for token t . This single linear projection is the standard router parameterization in modern open-weight MoE language models (Table 1). The standard top- k route is the index set of the k

Table 1: MoE language models used in our experiments. The expert column shows total / active experts per layer, with shared experts (always activated) listed after a ‘+’.

Model	Total / Active Params	Layers	N / k
Qwen3-30B-A3B (Yang et al., 2025)	30.5B / 3.3B	48	128 / 8
GPT-OSS-20B (Agarwal et al., 2025)	21B / 3.6B	24	32 / 4
DeepSeek-V2-Lite (Liu et al., 2024a)	16B / 2.4B	27	64 / 6 + 2
OLMoE-1B-7B (Muennighoff et al., 2024)	7B / 1.3B	16	64 / 8

highest-scoring experts,

$$S_t^{\text{std}} = \text{TopK}(s_t, k) \subseteq \{1, \dots, N\}, \quad |S_t^{\text{std}}| = k, \quad (1)$$

where $k \ll N$ in practice, with $k = 8$ out of $N = 128$ in Qwen3-30B-A3B as a typical example.

Only the selected experts are executed. Their outputs are combined into the layer output by softmax-normalizing the router scores within S_t^{std} ,

$$h_t^{\text{std}} = \sum_{i \in S_t^{\text{std}}} g_{ti}^{\text{std}} E_i(x_t), \quad g_{ti}^{\text{std}} = \frac{\exp(s_{ti})}{\sum_{j \in S_t^{\text{std}}} \exp(s_{tj})}, \quad (2)$$

so that the gate weights g_{ti}^{std} form a distribution over S_t^{std} . Unselected experts contribute neither their outputs nor their scores to h_t^{std} . The next-token cross-entropy at position t , $C_t = -\log p_\theta(y_t | x, y_{<t})$ where y_t is the realized next token and θ collects all model parameters, is therefore a function of the standard route S_t^{std} alone when θ is fixed.

3 Evaluating Routing Quality

Given a trained MoE language model, we ask whether its router selects expert sets that are really useful for the tokens it routes. We answer this by comparing the standard top- k route against sampled alternatives for the same token. Section 3.1 describes the analysis protocol, including how we sample alternative routes and measure their utility. Section 3.2 reports our main finding: the standard router is well-aligned with route utility on confident tokens, but this alignment collapses on harder tokens, where the standard route is rarely among the lowest-loss candidates. Section 3.3 shows that this pattern persists across MoE layers, evaluation domains, and model families.

3.1 Analysis Protocol

Setup. We analyze four open-weight MoE language models (Table 1) on verified self-generated reasoning trajectories. Our primary analysis uses Qwen3-30B-A3B on MATH Level-5 (Hendrycks et al., 2021); we extend to the other models and to AIME, HMMT, and GPQA-Diamond (Rein et al., 2023) in Section 3.3. For each problem we sample candidate solutions and retain one verified-correct trajectory $y_{1:T}$ generated under prompt x , restricted to assistant-response tokens.

Sampled alternative routes. For token t at MoE layer ℓ , let $S_{t,\ell}^{\text{std}}$ denote the standard top- k route. We form a candidate expert pool $P_{t,\ell}$ consisting of the $m = 32$ highest-scoring routed experts under the trained router at that token and layer. We compare the standard route against $G = 32$ equal-compute alternatives drawn within this pool via Gumbel-top- k sampling: for each $g = 1, \dots, G$, we draw independent Gumbel noise $\epsilon^{(g)} \sim \text{Gumbel}(0, 1)^m$ and take $S_{t,\ell}^{(g)} = \text{TopK}_{i \in P_{t,\ell}}(s_{t,\ell,i} + \epsilon^{(g)}, k)$. This yields a candidate set $\mathcal{A}_{t,\ell} = \{S_{t,\ell}^{\text{std}}, S_{t,\ell}^{(1)}, \dots, S_{t,\ell}^{(G)}\}$ of $G + 1 = 33$ routes. For each $S \in \mathcal{A}_{t,\ell}$, we intervene at (t, ℓ) by replacing the standard route with S , recompute the gate weights, and run the rest of the model forward with all other parameters fixed.

Routing-quality metrics. Recent work has shown that a small subset of pivotal tokens disproportionately determines reasoning success (Abdin et al., 2024; Lin et al., 2024), and that local signals such as next-token entropy can identify them (Wang et al., 2025). We use trajectories that are verified correct, so each realized next token lies on a successful path; the probability a route assigns to this token is a necessary condition for routing well at t , and serves as a local proxy for routing quality.

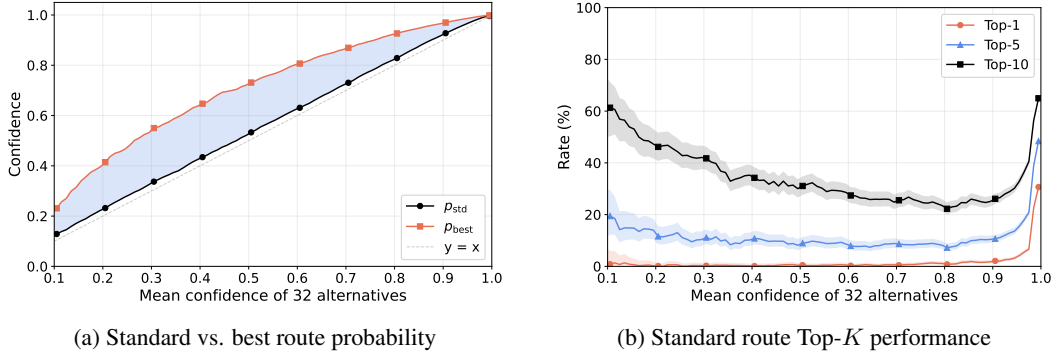


Figure 2: **Routing quality degrades sharply on low-confidence tokens.** (a) Standard route probability vs. best route probability across token difficulty, showing gap as tokens become harder. (b) Standard route performance measured by Top- K rates.

Based on this successful path, we report the standard-route probability $p_{t,\ell}(S^{std})$, the best-route probability $\max_S p_{t,\ell}(S)$, their gap, and the Top- K rates for $K \in \{1, 5, 10\}$, defined as the fraction of tokens at which the standard route ranks within the top K of the 33 candidates. We stratify tokens by route-averaged probability $\bar{p}_{t,\ell} = \frac{1}{G} \sum_{S \in \mathcal{A}_{t,\ell} \setminus \{S^{std}\}} p_{t,\ell}(S)$ into *Confident* $([0.9, 1])$, *Ambiguous* $([0.5, 0.9])$, and *Fragile* $([0, 0.5])$.

3.2 Routing Quality Degrades with Token Difficulty

We apply the protocol of Section 3.1 to Qwen3-30B-A3B at the final MoE layer on verified MATH Level-5 trajectories, comparing each standard route against $G = 32$ sampled equal-compute alternatives. The resulting statistics, stratified by token difficulty, are summarized in Figure 2.

In Figure 2a, the standard-route probability tracks the route-averaged probability $\bar{p}_{t,\ell}$ closely across the full range. On Confident tokens, this is not a demanding test of routing quality: all evaluated routes already assign very high probability to the realized next token, so the difference between the standard route and the best evaluated route is negligible. In this regime, routing choice has little observable consequence. The important behavior appears once $\bar{p}_{t,\ell}$ leaves the Confident range. As tokens become Ambiguous or Fragile, the best evaluated route remains substantially above the standard route, showing that a same-compute alternative inside the frozen model assigns much higher probability to the successful continuation. Thus the failure is not uniform across tokens; it appears precisely where route choice begins to matter.

Figure 2b shows the same pattern in rank space. High Top- K rates on Confident tokens are expected because many routes already perform nearly perfectly. Outside this high-probability regime, however, the standard route’s rank collapses: Top-1, Top-5, and Top-10 rates drop sharply and remain near the floor. The router is therefore not merely missing small gains on easy tokens; it becomes uninformative on the tokens where alternative routes differ meaningfully in realized-token probability.

3.3 Consistency across Layers, Domains, and Models

The pattern in Section 3.2 is not specific to the final MoE layer of Qwen3-30B-A3B on MATH Level-5. We repeat the analysis along three axes: across other MoE layers within Qwen3-30B-A3B, across other reasoning and knowledge benchmarks, and across other MoE language models. The qualitative shape is preserved (Tables 2–4); only the magnitude varies, in interpretable ways.

Layers. We repeat the analysis at an early (L0), middle (L24), and final (L47) MoE layer of Qwen3-30B-A3B (Table 2). On Fragile tokens, the Top-1 rate is at or near the uniform baseline at all three layers, so the misalignment is not specific to the final layer. The Fragile-token gap, however, grows monotonically with depth (11.4, 12.8, 20.4), which is consistent with the fact that an error at the final MoE layer feeds directly into the next-token distribution with no further routing left to correct it. We accordingly focus on the final layer for the rest of the analysis and for the recovery experiment in Section 5.

Table 2: **Layer-wise routing quality.** L0, L24, L47 refer to early, middle, and final MoE layers respectively. Tokens are binned by route-averaged next-token probability. Gap shows probability improvement from standard to best route. All values are in percent.

Layer	Confident			Ambiguous			Fragile		
	L0	L24	L47	L0	L24	L47	L0	L24	L47
Tokens (%)	75.9	72.8	78.7	16.7	18.7	14.3	7.4	8.5	6.9
Top-1 (%)	34.8	21.9	51.9	4.1	2.6	1.5	4.1	2.9	0.8
Top-5 (%)	48.7	38.5	68.8	19.3	16.5	9.6	21.3	19.0	10.5
Top-10 (%)	61.4	55.4	80.5	36.8	36.0	26.5	40.5	40.7	36.7
p_{std} (%)	99.4	99.2	99.6	74.9	74.6	77.9	36.9	37.0	40.2
p_{best} (%)	99.7	99.6	99.8	83.4	83.9	88.9	48.3	49.8	60.6
Gap (pp)	0.3	0.4	0.2	8.5	9.3	11.0	11.4	12.8	20.4

Table 3: **Routing quality across reasoning and knowledge benchmarks.** AIME pools 2024 and 2025 (10 trajectories), HMMT 2025 (10 trajectories), and GPQA-Diamond (100 trajectories). Conf., Amb., and Frag. denote the Confident, Ambiguous, and Fragile bins, respectively.

Benchmark	AIME			HMMT			GPQA		
	Conf.	Amb.	Frag.	Conf.	Amb.	Frag.	Conf.	Amb.	Frag.
Tokens (%)	71.6	17.9	10.5	74.6	16.3	9.2	78.2	16.4	5.5
Top-1 (%)	40.8	1.2	0.6	44.4	1.3	0.7	40.3	2.6	1.6
Top-5 (%)	63.2	10.2	11.9	63.6	8.7	10.4	58.9	12.1	14.0
Top-10 (%)	75.8	26.8	37.5	76.3	24.3	37.0	75.4	31.6	44.6
p_{std} (%)	99.5	77.6	37.4	99.5	76.9	37.5	99.6	79.4	50.0
p_{best} (%)	99.8	88.2	56.8	99.8	87.9	56.5	99.8	90.5	71.2
Gap (pp)	0.3	10.6	19.4	0.3	11.0	19.0	0.2	11.1	21.2

Table 4: **Routing quality across MoE language models.** Each model is evaluated with its native top- k configuration.

Model	GPT-OSS			DeepSeek			OLMoE		
	Conf.	Amb.	Frag.	Conf.	Amb.	Frag.	Conf.	Amb.	Frag.
Tokens (%)	71.8	15.4	12.8	67.0	21.1	11.9	52.5	32.7	14.8
Top-1 (%)	13.9	2.9	1.8	4.6	1.1	0.6	43.0	23.9	6.4
Top-5 (%)	46.0	22.3	23.7	18.0	5.8	5.1	84.1	58.9	27.8
Top-10 (%)	65.9	42.1	44.8	46.2	23.2	26.2	95.8	80.9	59.0
p_{std} (%)	99.2	75.9	26.2	99.5	85.6	42.6	99.9	95.3	57.3
p_{best} (%)	99.6	85.9	38.1	99.8	94.3	67.5	99.9	98.2	78.1
Gap (pp)	0.4	9.9	11.8	0.3	8.7	24.9	0.1	2.9	20.8

Domains. We extend the analysis to AIME, HMMT, and GPQA-Diamond on Qwen3-30B-A3B at the final MoE layer (Table 3). On AIME and HMMT, both math-heavy benchmarks like MATH Level-5, the qualitative pattern of Section 3.2 holds: Fragile tokens have low standard-route probability (~ 37), large best-route gaps (~ 19), and very low Top-1 rates (0.6, 0.7). GPQA-Diamond shows the same qualitative pattern but less severe: the Fragile fraction is smaller (5.5 vs ~ 10), the standard-route probability on Fragile tokens (50.0) and the Top-1 rate (1.6) are higher. The best-route gap is comparable in magnitude (21.2).

Models. We repeat the MATH Level-5 analysis on GPT-OSS-20B, DeepSeek-V2-Lite, and OLMoE-1B-7B at each model’s final MoE layer using its native top- k configuration (Table 4). The qualitative pattern of Section 3.2 holds across all three: the standard router is well-aligned on Confident tokens and substantially less so on Fragile ones, with Fragile-token best-route gaps of 11.8, 24.9, and 20.8 respectively. Absolute levels differ across models: OLMoE-1B-7B keeps higher Top- K rates throughout, including on Fragile tokens, while DeepSeek-V2-Lite has very low Top-1 rates even on Confident tokens. But in every case the standard route stops tracking route utility once $\bar{p}_{t,\ell}$ leaves the Confident range. The consistency of this pattern across model families, layers, and domains points to a shared cause that does not depend on which particular router was trained.

4 A Counterfactual Blind Spot in Standard MoE Training

The shared cause lies in how standard top- k MoE training evaluates routing decisions. The language modeling loss measures only the loss of the route that was executed, and load balancing losses depend only on aggregate router-side statistics. Neither places a token-level signal on equal-compute routes that were not executed. We call this gap the counterfactual blind spot. The blind spot predicts the empirical signature observed in Section 3. Routing decisions are well-trained where their utility is identifiable from the executed loss, and progressively less informative as that identifiability degrades.

4.1 Formalizing the Blind Spot

It is well documented that token-to-expert routing in MoE language models stabilizes early in training and changes little thereafter (Dai et al., 2022; Xue et al., 2024). The structure of the language-modeling objective explains why. For a token t , only the executed route S_t^{std} enters the forward pass, so differentiating C_t with respect to a router score s_{tj} within a fixed top- k cell yields

$$\frac{\partial C_t}{\partial s_{tj}} = \mathbf{1}\{j \in S_t^{\text{std}}\} g_{tj}^{\text{std}} \left(\nabla_{h_t^{\text{std}}} C_t \cdot (E_j(x_t) - h_t^{\text{std}}) \right). \quad (3)$$

The indicator is the key term. For $j \in S_t^{\text{std}}$, the gradient refines the scores and gate weights of the experts already in the executed mixture; for $j \notin S_t^{\text{std}}$, it vanishes, and the unselected expert’s output $E_j(x_t)$ never enters the computation graph. Two distinct routes $S, S' \subseteq \{1, \dots, N\}$ with $|S| = |S'| = k$ produce different next-token cross-entropies $C_t(S)$ and $C_t(S')$ on the same token, but standard training observes only one of them.

This is not a gradient bug but the intended sparse computation; the point is that the resulting signal fine-tunes routing within the executed top- k cell while leaving routes in neighboring cells unevaluated. Because the standard router is a single linear projection across the MoE models, there is no separate router-side mechanism that can infer these missing counterfactual losses without an additional training signal. The known stability of trained routing decisions then has a structural reading: once an early routing pattern is established, the gradient signal fine-tunes that pattern but cannot, on its own, propose a better one for tokens where the pattern routes poorly.

4.2 Load Balancing Does Not Provide Token-Level Counterfactual Signal

A natural question is whether the load-balancing losses used in MoE pretraining mitigate this blind spot. They can: by discouraging expert collapse, load balancing encourages broader expert coverage and can cause underused experts to be executed more often during training. However, this aggregate exploration is not the same as token-level counterfactual supervision. We call a load-balancing regularizer aggregate if its value and gradient depend only on router scores, router probabilities, and aggregate routing statistics, rather than on the expert outputs $\{E_j(x_t)\}$ or the cross-entropies $\{C_t(S)\}$ that would result from executing alternative routes on token t . Such a regularizer may change which experts are explored across a batch, but it does not tell the router which equal-compute alternative would have lowered the loss on a particular hard token.

We make this concrete for the Switch-style load-balancing loss (Fedus et al., 2022), a widely-used variant in MoE training. For a batch of T tokens, let $p_t = \text{softmax}(s_t) \in \Delta^{N-1}$ and define

$$f_i = \frac{1}{Tk} \sum_{t=1}^T \mathbf{1}\{i \in S_t^{\text{std}}\}, \quad \bar{p}_i = \frac{1}{T} \sum_{t=1}^T p_{ti}, \quad (4)$$

the fraction of routed slots assigned to expert i and its average router probability, with the Switch-style loss given by $R_{\text{lb}} = \lambda N \sum_i f_i \bar{p}_i$. Treating f as fixed, as is standard given the non-differentiability of the routed indicator, only \bar{p} depends differentiably on s_t , and the softmax Jacobian gives

$$\nabla_{s_t} R_{\text{lb}} = \frac{\lambda N}{T} (\text{diag}(p_t) - p_t p_t^\top) f. \quad (5)$$

This gradient depends only on f and p_t but not on $\{E_j(x_t)\}$ or $\{C_t(S)\}$, confirming that the Switch-style loss is aggregate in the sense defined above. The same property holds for the other variants used in current open-weight MoE models: the Importance and Load losses of Shazeer et al. (2017), the

GShard auxiliary loss (Lepikhin et al., 2020), the device-level balance terms of Liu et al. (2024a), and the auxiliary-loss-free bias update of Wang et al. (2024a) adopted in Liu et al. (2024b). These mechanisms are important for preventing expert collapse and improving aggregate coverage, but they do not directly supply the missing counterfactual route-loss signal. Closing the blind spot studied here would require a signal that compares the loss of the executed route with the losses of alternative equal-compute routes for the same token.

5 Probing the Routing Blind Spot with a Minimal Update

Section 4 left the two mechanisms underlying high-loss tokens mixed: intrinsic difficulty and routing failure both contribute, and the executed-route loss alone cannot tell them apart. We now partially separate them by intervening only on routing inside the frozen model. If a minimal router-only update is sufficient to shift downstream pass@ K , then at least part of the high loss on hard tokens is reachable by re-routing alone rather than requiring expert re-training. Concretely, we update only the final-layer router while leaving every expert and every other router frozen. At evaluation time, the model uses ordinary top- k routing (with updated parameters) with no test-time search.

5.1 Expert Preference Optimization

Method. To this end, we propose Expert Preference Optimization (EPO), a minimal router-only update that intervenes only on routing inside the frozen model. At each training step, we define hard tokens as tokens whose current next-token cross-entropy under the trainable router π_θ exceeds $\tau = 0.1$. For each such token t , let r_t^- be the top- k route currently selected by π_θ . We sample G alternative top- k routes from π_θ via Gumbel-top- k , all with the same number of routed experts as r_t^- . For each sample we recompute the gate weights, execute that route at the final MoE layer, and measure the resulting next-token cross-entropy with all other parameters fixed. If the lowest-CE sample improves over r_t^- , we use it as the chosen route r_t^+ ; otherwise the token contributes no gradient at this step.

Let π_{ref} denote the frozen standard router and π_θ the trainable router, initialized from π_{ref} . We treat each route r as a sequence of experts and use the factorized log-probability $\log \pi(r | x_t) = \sum_{e \in r} \log \pi(e | x_t)$, where $\pi(e | x_t)$ is the router softmax probability assigned to expert e . We then train π_θ with a CE-gap-weighted DPO-style objective (Amini et al., 2024; Zhou et al., 2024):

$$\ell_t = -\Delta_t \log \sigma \left(\beta \log \frac{\pi_\theta(r_t^+ | x_t)}{\pi_{\text{ref}}(r_t^+ | x_t)} - \beta \log \frac{\pi_\theta(r_t^- | x_t)}{\pi_{\text{ref}}(r_t^- | x_t)} \right), \quad (6)$$

where $\Delta_t = \max(0, C(r_t^-) - C(r_t^+))$ is the observed CE-gap weight.

Since r_t^+ and r_t^- have the same cardinality, shared experts cancel in the route log-probability difference and the softmax normalizers cancel as well. The update therefore acts only on experts that distinguish r_t^+ from r_t^- : chosen-only experts are pushed up, rejected-only experts are pushed down. EPO modifies the final-layer routing weights for the experts that separate a lower-loss route from the route currently chosen by the trainable router, without updating any expert weights.

Setup. We evaluate EPO on Qwen3-30B-A3B (Yang et al., 2025) and GPT-OSS-20B (Agarwal et al., 2025). We construct router-update data from MATH Level-5 (Hendrycks et al., 2021): for each problem we sample four solutions from the standard model and keep problems with at least one verified-correct solution, yielding approximately 2K verified trajectories. The hard-token filter described above is applied at each training step on these trajectories. We evaluate on AIME 2024+2025 and HMMT 2025 with the same decoding settings and number of samples per problem for both standard and EPO models.

5.2 Pass@K Shifts under a Router-Only Probe

Shifts under the router-only update. As illustrated in Figure 3, the standard and EPO curves are close on both benchmarks and both models, but the EPO curves sit above the standard curves at most reported K , and the 95% bootstrap bands separate from the standard over part of the reported range. The shifts are small and we read them as a minimal existence check rather than as a routing improvement method: a router-only update on the order of 0.001% of model parameters, with no

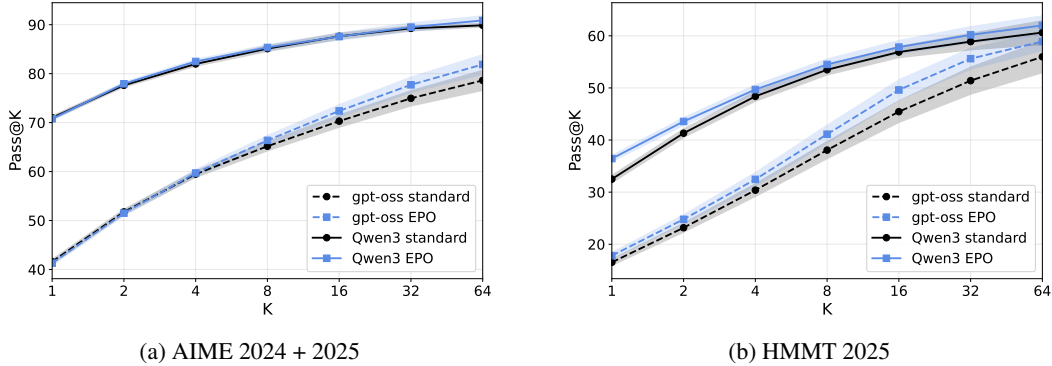


Figure 3: **Pass@K curves on AIME 2024+2025 and HMMT 2025.** For each problem, we pool $n = 160$ completions and compute $\text{pass}@K$ with the standard combinatorial estimator $\hat{q}_p(K) = 1 - \binom{n-c_p}{K} / \binom{n}{K}$, where c_p is the number of correct completions. Scores are averaged over problems. Shaded bands show 95% bootstrap confidence intervals; see Appendix C for details.

Table 5: **EPO’s effect on routing quality.** A: standard trajectory with the pre-trained router. B: standard trajectory with EPO-updated router. C: EPO trajectory with EPO-updated router.

	Confident			Ambiguous			Fragile		
	A	B	C	A	B	C	A	B	C
Tokens (%)	73.2	74.5	75.8	17.0	16.0	16.0	9.8	9.6	8.2
Top-1 (%)	42.7	27.0	26.3	1.2	2.4	1.9	0.6	1.9	2.4
Top-5 (%)	63.4	43.5	43.3	9.4	16.8	16.2	11.2	17.9	20.7
Top-10 (%)	76.1	60.6	61.1	25.5	35.7	35.7	37.2	39.7	44.5
p_{std} (%)	99.5	99.4	99.5	77.2	77.7	77.9	37.5	35.0	39.0
p_{best} (%)	99.8	99.8	99.8	88.1	89.2	89.3	56.6	56.8	59.5
Gap (pp)	0.3	0.3	0.3	10.8	11.5	11.3	19.2	21.9	20.5

expert or attention block modified, is sufficient to move $\text{pass}@K$ above the standard curve under bootstrap uncertainty. We interpret this as evidence that part of the high loss on hard tokens is reachable inside the frozen model by re-routing alone, rather than requiring expert re-training.

Where does the shift come from? Table 5 decomposes EPO’s effect by separately varying the router used for ordinary top- k selection and the trajectory being analyzed. ‘A’ is the standard baseline. ‘B’ holds the generated trajectory fixed and evaluates the EPO router, isolating how the updated router changes route selection on the standard-model trajectory. ‘C’ uses the EPO router end-to-end, capturing both changed routing and the resulting change in generated trajectories. First, EPO shifts the token distribution toward easier bins: the Confident fraction increases from 73.2 in A to 74.5 in B and 75.8 in C, while the Fragile fraction decreases from 9.8 to 9.6 and then 8.2. Second, the route-rank gains occur mainly outside the Confident bin. On Ambiguous tokens, A \rightarrow B raises Top-1 from 1.2 to 2.4, with corresponding gains in Top-5 and Top-10. On Fragile tokens, Top-1 rises from 0.6 in A to 1.9 in B and 2.4 in C, again with Top-5 and Top-10 improving as well.

Interpreting the Confident-bin rank drop. The decline of Top- K rates on Confident tokens should be interpreted differently. In this bin, route choice has little measurable effect: p_{std} remains around 99.5, p_{best} around 99.8, and the Gap stays at only 0.3 percentage points across A, B, and C. Thus the lower Confident-bin rank rates do not indicate a meaningful loss in next-token probability. Rather, EPO appears to reduce an easy-token-biased rank alignment of the original router, while improving rank alignment on Ambiguous and Fragile tokens where different equal-compute routes lead to substantially different realized-token probabilities. We therefore interpret Table 5 as evidence that the router-only update changes route selection in the regimes where route choice matters, while leaving already-confident predictions essentially unchanged at the probability level.

6 Related Work

MoE training. A large body of work makes sparse routing scalable, balanced, and stable during pretraining. Auxiliary load-balancing losses prevent expert collapse (Shazeer et al., 2017; Lepikhin et al., 2020; Fedus et al., 2022), auxiliary-loss-free balancing replaces these with bias updates from observed expert load (Wang et al., 2024a), and the router z -loss controls router logit magnitudes for stability (Zoph et al., 2022). A separate line modifies the routing rule itself (Lewis et al., 2021; Zhou et al., 2022; Puigcerver et al., 2023; Wang et al., 2024c). After pretraining, MoE-specific methods adapt task-relevant experts (Wang et al., 2024b), use route exploration as an RL signal for the router (Kim and Kang, 2025), constrain routing drift during fine-tuning (Kim et al., 2025), or incorporate expert selection into RL post-training (Ko et al., 2026; Ma et al., 2026). These works improve how routing is learned or adapted, but none directly evaluates whether the routes selected by a trained top- k router are counterfactually good.

Token-level analysis of reasoning. Reasoning success is determined disproportionately by a small subset of tokens: pivotal tokens have outsized effect on final-answer correctness (Abdin et al., 2024), intervening on critical tokens identified by token-level contrastive estimation substantially changes reasoning outcomes (Lin et al., 2024), and high-entropy minority tokens drive most of the policy improvement during RL training (Wang et al., 2025). Our Fragile bin is not identical to these prior definitions of pivotal, critical, or high-entropy tokens. It is a route-conditional diagnostic: a token is Fragile when sampled equal-compute routes assign low average probability to the realized continuation. The connection is therefore conceptual rather than operational. Both lines of evidence suggest that aggregate token averages can hide failures concentrated on a small number of uncertain positions, where local decisions may matter disproportionately.

Analyzing routing in trained MoE. Prior analyses of trained MoE models document expert specialization, routing saturation, and domain or vocabulary structure (Xue et al., 2024; Muennighoff et al., 2024). These ask what routing has learned, framed as which expert receives which token. We ask an orthogonal question: given the route the router selected, was it a good choice relative to other equal-compute routes inside the same frozen model. A router can route consistent token types to consistent experts and still select a suboptimal expert set on the tokens that matter most. A separate line intervenes on routing at inference time, by sampling from uncertain expert choices (Chen et al., 2026), pruning or reinforcing experts without retraining (Chen et al., 2025), or optimizing expert mixtures per input (Li et al., 2025a,b). These also treat the default route as not necessarily optimal, with Chen et al. (2026) in particular tying the intervention to token-level uncertainty. Our analysis is upstream: we measure whether the default route is counterfactually good in the first place, under the frozen model and without test-time search.

7 Conclusion

We analyzed routing quality in trained MoE language models by comparing each standard top- k route against sampled equal-compute alternatives under the frozen model. The standard router is well-aligned with route utility on confident tokens but uninformative on the fragile tokens that drive hard reasoning, and this token-conditional pattern holds across four open-weight MoE families. The pattern is consistent with a structural property of standard top- k training: the language modeling loss evaluates only the executed route, and load balancing depends only on aggregate routing statistics, so neither places a token-level signal on the equal-compute routes that were not selected. A minimal router-only update on hard tokens is sufficient to shift downstream pass@ K on mathematical reasoning tasks, indicating that the failure reflects misallocation reachable by the router alone rather than a pure capacity limit. We take these results to suggest that aggregate routing metrics are not sufficient to detect failures of routing quality, and that routing on hard tokens warrants attention as a target of MoE training rather than as an implementation detail of sparsity.

Limitations. We analyze each layer’s routing independently, holding the other layers fixed; whether per-layer failures compound or cancel when routing is modified jointly across layers is a separate question we do not address. Our analysis also restricts attention to verified-correct trajectories, where the realized next token already lies on a successful path; we use its probability under route

intervention as a proxy for routing quality on hard tokens, but this proxy may overstate the room for improvement on tokens where the realized token was itself a fortunate sample.

From diagnosis to prevention. Our analysis is performed on already-trained MoE models, but the failure it documents is a property of how these models are trained: standard top- k pretraining provides no token-level signal on routes that were not executed, and the misalignment we observe at fragile tokens is the predictable consequence. The natural follow-up is therefore not to refine the post-hoc router-only update, but to address the cause at training time. Concretely, this means designing a pretraining objective that places token-level signal on equal-compute alternative routes, for example by lightweight evaluation of sampled alternative routes alongside the executed one and incorporating their cross-entropies into the loss. Whether such a counterfactual-aware objective can be implemented at pretraining scale without sacrificing the efficiency advantages of sparse computation, and whether routers trained under it avoid the difficulty-conditioned failure documented here in the first place, are the questions our analysis points to.

References

- Abdin, M., Aneja, J., Behl, H., Bubeck, S., Eldan, R., Gunasekar, S., Harrison, M., Hewett, R. J., Javaheripi, M., Kauffmann, P., et al. (2024). Phi-4 technical report. *arXiv preprint arXiv:2412.08905*.
- Agarwal, S., Ahmad, L., Ai, J., Altman, S., Applebaum, A., Arbus, E., Arora, R. K., Bai, Y., Baker, B., Bao, H., et al. (2025). gpt-oss-120b & gpt-oss-20b model card. *arXiv preprint arXiv:2508.10925*.
- Amini, A., Vieira, T., and Cotterell, R. (2024). Direct preference optimization with an offset. In *Findings of the Association for Computational Linguistics: ACL 2024*, pages 9954–9972.
- Chen, Y., Wang, P., Shao, Y., and Cheng, J. (2025). Ban&pick: Achieving free performance gains and inference speedup via smarter routing in moe-llms. *arXiv e-prints*, pages arXiv–2509.
- Chen, Y., Wang, P., Zeng, N., Shao, Y., Li, G., Liu, J., and Cheng, J. (2026). Certain head, uncertain tail: Expert-sample for test-time scaling in fine-grained moe. *arXiv preprint arXiv:2602.02443*.
- Dai, D., Dong, L., Ma, S., Zheng, B., Sui, Z., Chang, B., and Wei, F. (2022). Stablemoe: Stable routing strategy for mixture of experts. *arXiv preprint arXiv:2204.08396*.
- Du, N., Huang, Y., Dai, A. M., Tong, S., Lepikhin, D., Xu, Y., Krikun, M., Zhou, Y., Yu, A. W., Firat, O., et al. (2022). Glam: Efficient scaling of language models with mixture-of-experts. In *International conference on machine learning*, pages 5547–5569. PMLR.
- Fedus, W., Zoph, B., and Shazeer, N. (2022). Switch transformers: Scaling to trillion parameter models with simple and efficient sparsity. *Journal of Machine Learning Research*, 23(120):1–39.
- Guo, D., Yang, D., Zhang, H., Song, J., Wang, P., Zhu, Q., Xu, R., Zhang, R., Ma, S., Bi, X., et al. (2025). Deepseek-r1: Incentivizing reasoning capability in llms via reinforcement learning. *arXiv preprint arXiv:2501.12948*.
- Hendrycks, D., Burns, C., Kadavath, S., Arora, A., Basart, S., Tang, E., Song, D., and Steinhardt, J. (2021). Measuring mathematical problem solving with the math dataset. *arXiv preprint arXiv:2103.03874*.
- Jiang, A. Q., Sablayrolles, A., Roux, A., Mensch, A., Savary, B., Bamford, C., Chaplot, D. S., Casas, D. d. l., Hanna, E. B., Bressand, F., et al. (2024). Mixtral of experts. *arXiv preprint arXiv:2401.04088*.
- Kim, G. and Kang, S. (2025). Exploration-driven reinforcement learning for expert routing improvement in mixture-of-experts language models. In *Findings of the 2025 Conference on Empirical Methods in Natural Language Processing*.
- Kim, J., Song, M., Shin, S., and Son, S. (2025). Defending moe llms against harmful fine-tuning via safety routing alignment. *arXiv preprint arXiv:2509.22745*.
- Ko, D., Park, J., Choi, S., Lee, S., Lee, S., and Kim, H. J. (2026). Moe-grpo: Optimizing mixture-of-experts via reinforcement learning in vision-language models. *arXiv preprint arXiv:2603.24984*.

- Lepikhin, D., Lee, H., Xu, Y., Chen, D., Firat, O., Huang, Y., Krikun, M., Shazeer, N., and Chen, Z. (2020). Gshard: Scaling giant models with conditional computation and automatic sharding. *arXiv preprint arXiv:2006.16668*.
- Lewis, M., Bhosale, S., Dettmers, T., Goyal, N., and Zettlemoyer, L. (2021). Base layers: Simplifying training of large, sparse models. In *International Conference on Machine Learning*, pages 6265–6274. PMLR.
- Li, Z., Li, Z., and Zhou, T. (2025a). C3po: Critical-layer, core-expert, collaborative pathway optimization for test-time expert re-mixing. *arXiv preprint arXiv:2504.07964*.
- Li, Z., Li, Z., and Zhou, T. (2025b). R2-t2: Re-routing in test-time for multimodal mixture-of-experts. *arXiv preprint arXiv:2502.20395*.
- Lin, Z., Liang, T., Xu, J., Lin, Q., Wang, X., Luo, R., Shi, C., Li, S., Yang, Y., and Tu, Z. (2024). Critical tokens matter: Token-level contrastive estimation enhances llm’s reasoning capability. *arXiv preprint arXiv:2411.19943*.
- Liu, A., Feng, B., Wang, B., Wang, B., Liu, B., Zhao, C., Deng, C., Ruan, C., Dai, D., Guo, D., et al. (2024a). Deepseek-v2: A strong, economical, and efficient mixture-of-experts language model. *arXiv preprint arXiv:2405.04434*.
- Liu, A., Feng, B., Xue, B., Wang, B., Wu, B., Lu, C., Zhao, C., Deng, C., Zhang, C., Ruan, C., et al. (2024b). Deepseek-v3 technical report. *arXiv preprint arXiv:2412.19437*.
- Ma, C., Huang, Z., Zeng, X., Wang, Y., Liang, C., Tian, K., Zhao, X., and Wang, L. (2026). Balancing the experts: Unlocking lora-moe for grpo via mechanism-aware rewards. In *The Fourteenth International Conference on Learning Representations*.
- Muennighoff, N., Soldaini, L., Groeneveld, D., Lo, K., Morrison, J., Min, S., Shi, W., Walsh, P., Tafjord, O., Lambert, N., et al. (2024). Olmoe: Open mixture-of-experts language models. *arXiv preprint arXiv:2409.02060*.
- Puigcerver, J., Riquelme, C., Mustafa, B., and Houlsby, N. (2023). From sparse to soft mixtures of experts. *arXiv preprint arXiv:2308.00951*.
- Rein, D., Hou, B. L., Stickland, A. C., Petty, J., Pang, R. Y., Dirani, J., Michael, J., and Bowman, S. R. (2023). Gpqa: A graduate-level google-proof q&a benchmark. *arXiv preprint arXiv:2311.12022*.
- Shazeer, N., Mirhoseini, A., Maziarz, K., Davis, A., Le, Q., Hinton, G., and Dean, J. (2017). Outrageously large neural networks: The sparsely-gated mixture-of-experts layer. *arXiv preprint arXiv:1701.06538*.
- Wang, L., Gao, H., Zhao, C., Sun, X., and Dai, D. (2024a). Auxiliary-loss-free load balancing strategy for mixture-of-experts. *arXiv preprint arXiv:2408.15664*.
- Wang, S., Yu, L., Gao, C., Zheng, C., Liu, S., Lu, R., Dang, K., Chen, X., Yang, J., Zhang, Z., et al. (2025). Beyond the 80/20 rule: High-entropy minority tokens drive effective reinforcement learning for llm reasoning. *arXiv preprint arXiv:2506.01939*.
- Wang, Z., Chen, D., Dai, D., Xu, R., Li, Z., and Wu, Y. (2024b). Let the expert stick to his last: Expert-specialized fine-tuning for sparse architectural large language models. In *Proceedings of the 2024 Conference on Empirical Methods in Natural Language Processing*, pages 784–801.
- Wang, Z., Zhu, J., and Chen, J. (2024c). Remoe: Fully differentiable mixture-of-experts with relu routing. *arXiv preprint arXiv:2412.14711*.
- Xue, F., Zheng, Z., Fu, Y., Ni, J., Zheng, Z., Zhou, W., and You, Y. (2024). Openmoe: An early effort on open mixture-of-experts language models. *arXiv preprint arXiv:2402.01739*.
- Yang, A., Li, A., Yang, B., Zhang, B., Hui, B., Zheng, B., Yu, B., Gao, C., Huang, C., Lv, C., et al. (2025). Qwen3 technical report. *arXiv preprint arXiv:2505.09388*.

Zhou, W., Agrawal, R., Zhang, S., Indurthi, S. R., Zhao, S., Song, K., Xu, S., and Zhu, C. (2024). Wpo: Enhancing rlhf with weighted preference optimization. In *Proceedings of the 2024 Conference on Empirical Methods in Natural Language Processing*, pages 8328–8340.

Zhou, Y., Lei, T., Liu, H., Du, N., Huang, Y., Zhao, V., Dai, A. M., Le, Q. V., Laudon, J., et al. (2022). Mixture-of-experts with expert choice routing. *Advances in Neural Information Processing Systems*, 35:7103–7114.

Zoph, B., Bello, I., Kumar, S., Du, N., Huang, Y., Dean, J., Shazeer, N., and Fedus, W. (2022). St-moe: Designing stable and transferable sparse expert models. *arXiv preprint arXiv:2202.08906*.

A Model Details

We analyze four open-weight Mixture-of-Experts language models. For each model we use the instruction-tuned variant publicly released on Hugging Face (Qwen3-30B-A3B-Instruct-2507, gpt-oss-20b with reasoning effort set to low, DeepSeek-V2-Lite-Chat, and OLMoE-1B-7B-0125-Instruct), evaluated in its native top- k configuration without any additional fine-tuning except as described in Section 5.1.

B Hyperparameter Details

This appendix documents the hyperparameters used in the counterfactual routing analysis (Section 3) and in the router-only update (Section 5). Table 6 lists the analysis hyperparameters, which are shared across all four MoE models we study, with model-specific values given for top- k and the target layer. The pool size of 32 refers to the size of the candidate expert pool over which Gumbel-top- k samples are drawn: at each token we restrict alternative routes to the 32 experts with the highest router scores, then perturb their scores with Gumbel noise. Table 7 lists the router-only update hyperparameters separately for Qwen3-30B-A3B and GPT-OSS-20B.

Table 6: Hyperparameters for the counterfactual routing analysis (Section 3).

Parameter	Value	Description
G	32	Number of alternative routes per token
Pool size	32	Candidate expert pool size
k	8 / 4 / 6 / 8	top- k for Qwen3 / GPT-OSS / DSv2 / OLMoE
Noise scale	1.0	Gumbel scale parameter
Target layer	L47 / L23 / L26 / L15	Final MoE layer for Qwen3 / GPT-OSS / DSv2 / OLMoE
Random seed	42	For subsample reproducibility
dtype	bf16	Inference precision
Number of problems	100 / 10 / 10 / 100	Randomly sampled per benchmark (MATH-L5 / AIME / HMMT / GPQA-Diamond)

C Experimental Details

This appendix documents the data construction and evaluation procedures used in the routing-quality analysis (Section 3) and in the router-only update (Section 5). For both, we generate self-sampled solutions on MATH Level-5 problems, retain verified-correct trajectories using exact-answer matching after normalization, and restrict attention to assistant-response tokens. The router-only update uses 2,269 verified trajectories for Qwen3-30B-A3B and 2,162 for GPT-OSS-20B. At each training step, the hard-token filter selects tokens whose current cross-entropy under the trainable router exceeds the threshold τ in Table 7, and only these tokens contribute gradient at that step.

Pass@ K evaluation uses AIME 2024+2025 (60 problems) and HMMT February 2025 (30 problems). For each problem we generate $n = 160$ completions (32 samples per run, pooled across 5 runs with different random seeds), and compute the per-problem pass@ K with the unbiased combinatorial estimator $\hat{q}_p(K) = 1 - \binom{n-c_p}{K} / \binom{n}{K}$, where c_p is the number of correct completions. The reported pass@ K is the mean of $\hat{q}_p(K)$ across problems. To quantify the uncertainty of this mean, we apply

Table 7: Hyperparameters for the router-only update (Section 5).

Parameter	Qwen3-30B-A3B	GPT-OSS-20B
Target layer	L47	L23
Optimizer	AdamW	AdamW
Learning rate	3×10^{-4}	3×10^{-4}
Weight decay	0.01	0.01
β_{DPO}	0.1	0.1
Epochs	1	1
G	32	16
Pool size	32	16
k	8 (native)	4 (native)
Noise scale	1.0	1.0
Hard-token threshold τ	0.1	0.1
Batch size	16	16
Number of problems	2,269	2,162
Gradient norm clip	1.0	1.0
Random seed	42	42

parametric bootstrap (2,000 resamples) over the binomial sampling of c_p at $n = 160$: for each problem we draw $c_p^{(b)} \sim \text{Binomial}(n, c_p/n)$, recompute $\hat{q}_p^{(b)}(K)$, and average across problems to obtain a bootstrap replicate of the mean. The 95% confidence intervals shown as shaded bands in Figure 3 are the 2.5th and 97.5th percentiles of the 2,000 bootstrap replicates. Decoding settings are listed in Table 8.

Table 8: Decoding settings for AIME and HMMT pass@ K evaluation.

Setting	Qwen3-30B-A3B	GPT-OSS-20B
Temperature	0.6	1.0
top_p	0.95	0.95
top_k	—	20
Samples per problem	32×5 runs ($n = 160$)	32×5 runs ($n = 160$)
Max tokens	8192	8192
Reasoning effort	—	low

Compute. All experiments were conducted on NVIDIA RTX A6000 GPUs (48 GB). Qwen3-30B-A3B uses two A6000 GPUs and the other models (GPT-OSS-20B, DeepSeek-V2-Lite, OLMoE-1B-7B) each use a single A6000 GPU. Because the update procedure computes and stores gradients only for the router parameters, the GPU memory footprint is essentially that of the forward pass plus the model weights. Approximate wall-clock times for each experiment are listed in Table 9. The longer runtime for Qwen3-30B-A3B reflects inter-GPU communication overhead from sharding the model across two devices; running the same procedure on a single larger-memory GPU (e.g., A100 80 GB) would likely reduce wall-clock time substantially.

Table 9: Approximate wall-clock time per experiment.

Model	Routing-quality analysis	Router-only update
Qwen3-30B-A3B	2 hours	5 hours
GPT-OSS-20B	17 minutes	20 minutes
DeepSeek-V2-Lite	19 minutes	—
OLMoE-1B-7B	18 minutes	—

Software environment. Inference uses vLLM 0.10.1 with HuggingFace Transformers 4.57.6 on PyTorch 2.7.1 (Python 3.11). Pass@ K evaluation uses lighteval 0.13.0 and inspect_ai 0.3.202, with answer verification by exact-match comparison after standard normalization.